

Comparative study of transport properties of membranes based on graphene oxide prepared by Brodie and improved Hummers' methods

Ekaterina A. Chernova^{1,4,a}, Konstantin E. Gurianov^{1,b}, Victor A. Brotsman^{2,c}, Rishat G. Valeev^{3,d}, Olesya O. Kapitanova^{2,e}, Mikhail V. Berekchiian^{1,f}, Alexei V. Lukashin^{1,g}

¹Lomonosov Moscow State University, Faculty of Materials Science, Moscow, Russia

²Lomonosov Moscow State University, Faculty of Chemistry, Moscow, Russia

³Udmurt Federal Research Center of the Ural Branch of Russian Academy of Sciences, Izhevsk, Russia

⁴Tula State University, Tula, Russia

^achernova.msu@gmail.com, ^bgurianovke@yandex.ru, ^cbrotsman_va@mail.ru, ^drishatvaleev@mail.ru,

^eolesya.kapitanova@gmail.com, ^fmikhail.berekchiyan@yandex.ru, ^galexey.lukashin@gmail.com

Corresponding author: Ekaterina A. Chernova, chernova.msu@gmail.com

PACS 81.05.Rm, 47.56.+r

ABSTRACT A comparative study of transport characteristics of composite membranes based on graphene oxide prepared by Hummers' (H-GO) and Brodie (B-GO) methods is presented. By using Raman and XPS spectroscopy combined with gas and vapor measurements at non-zero pressure drop, it is shown that the difference in preparation methods results not only in different composition and microstructure of the membranes, but also in different water vapor permeability and resistance towards pressure drops during membrane performance. The H-GO samples are found to be more defective and stronger oxidized with C/O ratio of 1.8, whereas B-GO revealed a total C/O ratio of 2.6 with more perfect microstructure. The higher oxidation degree of H-GO membranes allows one to achieve higher water vapor permeability (up to ~170 Barrer at 100 % humidity) but dramatically lower stability towards pressure revealing the irreversible loss in permeability up to 46 % during the application of pressure drop of 1 bar. In contrast, B-GO membranes show slightly lower permeability (~140 Barrer at 100 % humidity) but enhanced pressure stability revealing the irreversible permeability loss of only 4 % at pressure drop of 1 bar which is about 10-fold smaller compared to H-GO stability. This could be explained by the difference in microstructural features of the H-GO and B-GO. Graphene oxide prepared by Hummer's method has more flexible and defective nanosheets, whereas Brodie's method gives rise to more rigid nanosheets with more perfect microstructure. The obtained results suggest that it is possible to prepare graphene oxide membranes with high resistance towards pressure using only the composition-microstructure interplay without additional modification with pressure-stabilizing agents.

KEYWORDS graphene oxide membranes, Hummers' method, Brodie method, oxidation degree, pressure stability, water vapor permeability

ACKNOWLEDGEMENTS The work is supported by the state program of world-class scientific and educational centers (assignment number FEWG-2021-0014) for the youth laboratory on the research direction "Studying gas permeability and physicochemical properties of sealing composite and carbon materials". The authors are grateful to Dr. Andrei Eliseev and his laboratory (Lomonosov Moscow State University) for help with experimental studies. The authors acknowledge shared services center "Surface and novel materials" of UdmFRC of UB RAS for XPS data acquisition.

FOR CITATION Chernova E.A., Gurianov K.E., Brotsman V.A., Valeev R.G., Kapitanova O.O., Berekchiian M.V., Lukashin A.V. Comparative study of transport properties of membranes based on graphene oxide prepared by Brodie and improved Hummers' methods. *Nanosystems: Phys. Chem. Math.*, 2023, **14** (2), 272–278.

1. Introduction

At present time, the dehydration of natural and technological gas mixtures has become one of the most important tasks in the conditioning of natural gas for pipeline transport, preparation of pure gases for electronics, chemical industry and medicine enterprises. To solve this problem, membrane technologies are developed, since the use of compact membrane modules can significantly reduce capital investments, and the energy intensity of the entire process. The key factors determining the effectiveness of membrane technology are the permeability and selectivity of the membrane material as well as its long-term stability and resistance towards external conditions including pressure drops. Currently, polymeric materials dominate in the membrane technological processes, however, they are prone to physical aging and plasticization

which significantly reduces both the performance and long-term stability of the membranes introducing challenges in design of membrane materials [1].

A reasonable alternative to polymers are carbon membranes, which are considered as advanced materials among with the graphene oxide (GO) and its modified derivatives [2]. Graphene oxide is a two-dimensional material which could be considered as a modification of graphene richly decorated with oxygen-containing groups, including hydroxyl, epoxy, carbonyl and carboxyl groups making GO a suitable candidate for dehumidification technologies. Graphene oxide is obtained by intercalation and oxidation steps of carbon precursors (commonly, graphite and carbon nanotubes) [2–4]. For industrial applications, the pressure stability of graphene oxide still remains an important issue. Generally, the permeability of GO-based membranes decreases with increasing operating pressure which is attributed to compaction of GO nanosheets and shrinking of interlayer spacing [5]. To enhance GO pressure stability, various pressure-resistant agents are introduced into interlayer galleries of GO. For instance, the layered carbon nitride (C_3N_4) nanoparticles [6], single-walled carbon nanotubes [7], functionalized fullerenes [8], zeolitic imidazolate framework particles [9] were reported to stabilize GO towards pressure drops. Moreover, the intercalation of positively charged copper hydroxide nanostrands [10] or K^+ ions [11] in GO were claimed even to increase water permeance with pressure. These results are promising, however, it is more desirable to manage the pressure stability using only intrinsic interplay of composition and microstructure in GO, because additional modification steps could strongly increase the complexity and costs of the graphene oxide membranes; moreover, the integration of foreign substances into GO matrix could inevitably induce the formation of additional structural defects. The stability of GO towards elevated pressures and pressure drops could be obviously based on the method of GO preparation. The understanding of this interrelation could give an opportunity to design the pressure-stable GO microstructure originally at the stage of its synthesis.

Four different classical methods are employed to obtain GO: the method of Brodie [12], Staudenmaier [13], Hoffman [14], and Hummers'/Offeman (or, simply, Hummers' method) [15]. The methods have a variety of modifications, for instance, at least, classical [15], modified [16] and improved Hummers' [3] methods have been reported. Each method of preparation endows the resulting GO with different chemistries making a strong impact on the microstructure and functional characteristics of GO membranes [17–19]. For instance, it was shown that Brodie-GO membranes reveal higher selectivity towards H_2 molecules due to a narrower interlayer spacing between GO nanosheets compared to Hummers' GO [18]. In other work, it was reported that, due to different chemistry, Brodie-GO is considered as a better photocatalytic platform than Hummers' GO [19]. It could be assumed that the difference in microstructure and chemistries of GO prepared by different methods could be employed for the enhancement of GO-based membranes for gas dehumidification without the need to modify GO with various pressure-resistant reagents.

In this work, a comparative analysis of the compositional and transport characteristics of membranes based on graphene oxide obtained by the improved Hummers' method (H-GO) [4] and Brodie method (B-GO) [5] is performed. The microstructure and chemical composition of the membranes is examined by scanning electron microscopy, Raman and X-ray photoelectron spectroscopy. The permeability of the membranes towards water vapors is studied under various humidity and pressure drops of the feed stream focusing on the possibility of pressure stability enhancement using only the interplay of microstructure and chemical composition of neat GO membranes. Our results present the general concept for improving functional properties of graphene oxide by careful choice of preparation method rather than post-modification with foreign substances.

2. Experimental part

Graphene oxide samples were obtained by improved Hummers' method and modified Brodie method. To prepare H-GO samples, graphite was oxidized by potassium permanganate with the graphite: $KMnO_4$ ratio of 1:6 [12]. The detailed description of the synthesis is presented in [6]. For the preparation of B-GO, potassium chlorate was used as an oxidant taking graphite/ $KClO_3$ ratio of 1:16. In a 100 ml flat-bottomed flask, 0.7 g of thermally expanded graphite and 9.6 g of potassium chlorate were added with constant stirring and cooling in an ice bath. To the resulting mixture, a fuming nitric acid was added dropwise (24.5 ml, one drop per second). The flask was left under constant stirring and room temperature for 12 hours, and then the reaction mixture was heated to $60\text{ }^\circ\text{C}$ and left for 8 hours at this temperature to further oxidize the graphite. As a result, the first batch of graphene oxide (B-GO1) was obtained. The resulting suspension was diluted with water in a ratio of 1:1 by volume, then the precipitate was separated by vacuum filtration and repeatedly washed with deionized water until the $pH = 6$. The precipitate was dried by sublimation and then subjected to re-oxidation as described above. The resulting mixture was stirred at $60\text{ }^\circ\text{C}$ for 20 hours. The obtained graphene oxide was repeatedly washed with deionized water until the $pH = 6$. For the purification from residual inorganic ions, the resulting H-GO and B-GO suspensions were subjected to dialysis for 30 days under constant stirring. The suspensions were further used for the formation of selective layers of composite membranes.

For composite membranes preparation, porous anodic aluminum oxide (AAO) membranes (pore diameter of ~ 80 nm, thickness $\sim 100\text{ }\mu\text{m}$) were used as reliable supports for GO thin selective layers. The AAO films preparation is described in [13, 14]: briefly, a standard anodic oxidation of aluminum foils with high purity (99.999 %) in $0.3\text{ M H}_2\text{C}_2\text{O}_4$ at 120 V was employed followed by selective removal of aluminum and etching of a barrier layer to get highly-permeable porous AAO supports with the N_2 permeance of $90 - 100\text{ m}^3\cdot\text{m}^{-2}\cdot\text{bar}^{-1}\cdot\text{h}^{-1}$ [15].

To obtain composite membranes, water-methanol suspensions with the concentration of 1 mg/ml were prepared by diluting the original H-GO and B-GO suspensions with methanol. The suspensions were carefully deposited on the surface of AAO supports by spin-coating at the rate of 1500 rpm. To achieve dense packing of the GO nanoflakes, vacuum suction was used upon the spin-coating and the several aliquots (30 – 50 mkl) of GO suspensions were deposited successively. To make sure that the obtained composite membranes have no large parasitic defects, the membranes were examined using optical microscope Carl Zeiss and tested for N_2 permeability.

To study the thickness and microstructure of the membranes, scanning electron microscopy (SEM) of membrane cross-sections was performed using Nvision 40 (Carl Zeiss) microscope. To get the average thickness of the selective layers, the SEM micrographs were statistically processed with ImageJ software.

To estimate the defectiveness of the H-GO and B-GO samples, the Raman spectroscopy was employed using a Renishaw InVia instrument with Leica DMLM optics (50 \times objective) and 20 mW 633 nm He-Ne laser. The obtained spectra were processed with Wire 3.4 Renishaw software, using Pseudo-Voigt functions positioned at 1340 ± 20 and $\sim 1590 \pm 10$ cm^{-1} for D- and G-peaks, respectively. Because graphene oxide is far more defective compared to graphene, the $I(D)/I(G)$ ratio for H-GO and B-GO was calculated using integrated areas of D and G peaks divided by their FWHM to get more reliable estimates of defectiveness.

To check the chemical composition of the membranes, X-ray photoelectron (XPS) spectra were registered on SPECS instrument by employing MgK- α excitation (excitation energy, $E_{ex} = 1254$ eV). Pure graphite C1s energy (284.6 eV) was used to calibrate the resulting spectra. The spectra were quantitatively processed with CasaXPS software using Shirley type background and mixed Gauss (70 %) – Lorentz (30 %) functions for spectra deconvolution. During the processing, the FWHM of spectral peaks was kept constant for all the spectral components. The subdivision of the C–C band into sp^2 -C, sp^3 -C-hybridized components was neglected due to an insufficient spectral resolution [16].

To study the transport characteristics of the membranes, a set of individual permanent gases (H_2 , N_2 , O_2 , CO_2 , CH_4 , C_4H_{10} and SF_6) was used. For the analysis, the membranes were tightened between a feed chamber and calibrated permeate chamber of a two-compartment measurement cell. Then, the permeate chamber was evacuated using a vacuum pump until the residual pressure of less than 0.1 mbar was achieved. After this, the stream of the measured gas was introduced into the feed chamber and a pressure-time curve was registered during the gas inflowing across the membrane into the permeate chamber. The fluxes of the permanent gases were calculated using a slope of the linear part of the pressure-time curve.

To study the water vapor permeability under a steady mode, a feed stream containing a mixture of dry N_2 and N_2 flux with controlled humidity was used. To obtain wet N_2 flux, the N_2 stream was bubbled through the vessel with liquid water. The control of the entire feed stream humidity was performed by setting the ratio of dry N_2 and wet N_2 fluxes. The feed stream was introduced to the feed side of the membrane, while the permeate side was blown with He flux (pressure = 1 bar). The permeability was measured under varied relative humidity of the feed stream (inlet relative humidity RH_{in}). For each humidity value, the membrane was blown with feed stream for at least 30 minutes to achieve an equilibrium steady flux across the membrane. During the experiment, the dependence of outlet relative humidity (RH_{out}) of the He flux was measured with time. The humidity and temperature of both gas fluxes were controlled using HHH-4000 sensors (Honeywell, USA). The experiments were performed at the temperatures of 23 – 25 $^{\circ}C$.

3. Results and discussion

The results of SEM have shown that the selective layers based on B-GO and H-GO are represented by thin and uniform layered films covering the entire surface of AAO supports. The average thickness of HGO- and BGO selective layers stands in the range 18 – 20 nm (Fig. 1(a,b)).

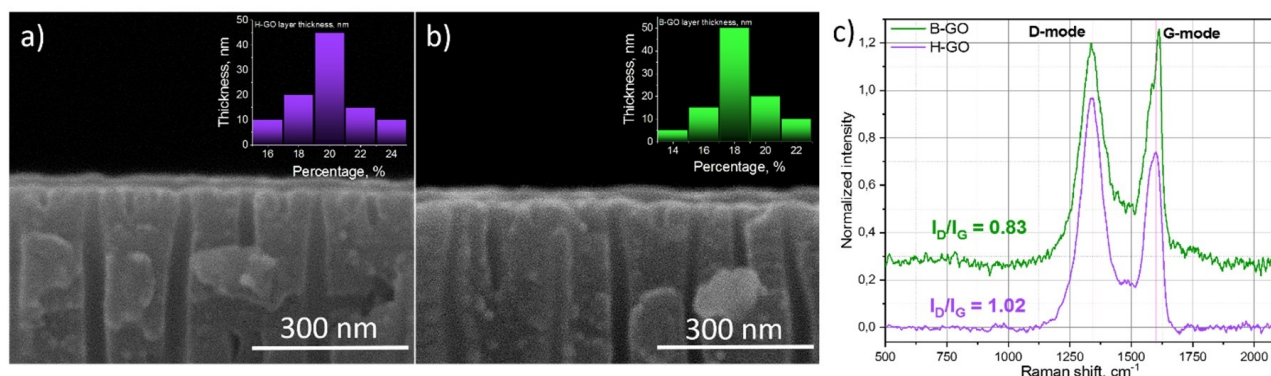


FIG. 1. SEM micrographs of cross-sections of the composite membranes with selective layers based on: a) H-GO; b) B-GO; c) Raman spectra for H-GO and B-GO membranes

Raman spectra of H-GO and B-GO show the typical D-mode (defect-activated peak coming from transverse optical phonons (TO phonons) with A_{1g} symmetry in graphene lattice) and G-mode (coming from optical phonon with E_{2g} -symmetry) (Fig. 1(c)). Generally, the D-peak is responsible for various types of defects in GO including sp^3 -carbons, edges, nanoflakes tilting, etc., whereas G-peak shows the vibrations of sp^2 -carbons in GO skeleton. It should be noted that graphene oxide is intrinsically sp^3 -rich and defective phase, and its Raman spectra are more complex containing D'' , D' , and D^* modes overlapping with apparently visible D and G peaks and making impact into peak areas [20,21]. At the same time, the ratio of intensities of D and G modes ($I(D)/I(G)$ ratio) are commonly used to estimate the defectiveness of carbon materials. In the present study, the $I(D)/I(G)$ ratio was calculated using heights of D and G peaks (see Experimental part) which gives one more reliable estimates for GO [20] rather than simple dividing of integrated areas of peaks commonly practiced in most of the works on graphene oxide. According to the results, it was revealed that B-GO sample has smaller $I(D)/I(G)$ ratio which could be estimated as lower level of defects in its structure compared to H-GO.

According to the XPS results (Fig. 2(a-d)), the GO sample obtained by improved Hummers' method is stronger oxidized achieving the C/O ratio of 1.8, whereas the C/O ratio of B-GO reaches 2.6, which is more close to mildly thermally-reduced GO [22]. Moreover, the ratio of single- to double- oxygen bonded carbon (C–O/C=O) reaches 4.0 for B-GO and only 2.8 for H-GO showing the strong and dominating contribution of C–O bonded groups (hydroxyls and epoxy groups) over C=O component (carbonyl, carboxyl groups) for graphene oxide obtained by the Brodie method (Fig. 2(e,f)). According to model structure of GO, the hydroxyl and epoxide groups are commonly located on the basal surface of GO nanoflakes [23]. Thus, B-GO membrane has less oxidized nanosheets with dominating presence of basal oxygen groups and is expected to be more rigid with smaller number of defects compared to H-GO-based membrane.

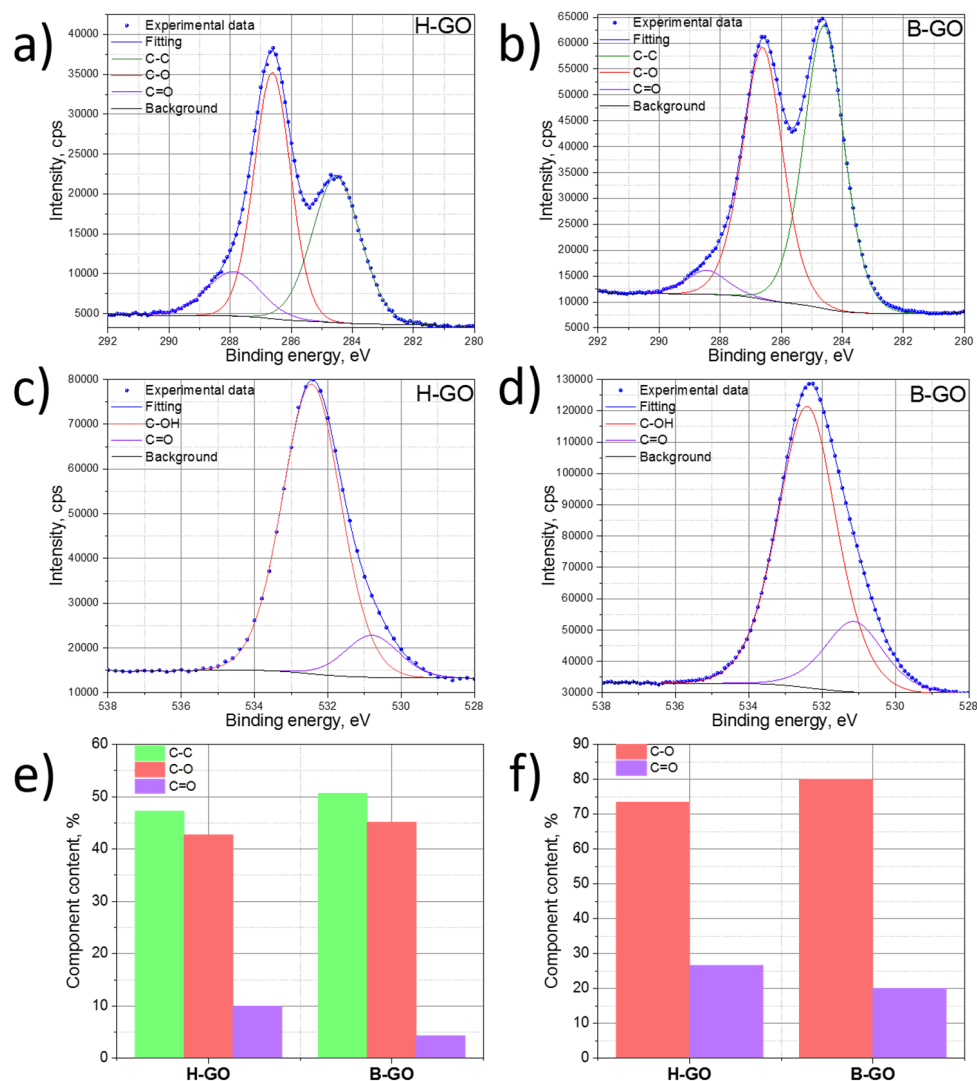


FIG. 2. XPS spectra of the composite membranes: a), c), and b), d), represent C1s spectra and O1s spectra for H-GO and B-GO samples, respectively; e),f) spectral components content calculated from C1s spectra (e), and O1s spectra (f) for H-GO and B-GO-based membranes

Both composite membranes based on H-GO and B-GO reveal low permeability towards permanent gases achieving the values not exceeding 0.002 – 0.003 Barrer for H_2 gas. Generally, there is a linear dependence of gas permeance on the inverse square root from molecular mass of gases obeying the Knudsen diffusion equation [24, 25].

Such a small permeability is achieved by dense packing of GO nanosheets upon spin-coating under vacuum suction, and favors a high potential for application of both H-GO and B-GO films in membrane technologies for selective gas dehumidification (Fig. 3(a)). It should be noted that B-GO membrane has smaller gas permeability compared to H-GO which could be attributed to more perfect structure of B-GO with smaller number of defects which stays in line with the Raman spectroscopy data. The results on gas permeability stay in good agreement with literature data suggesting nearly barrier gas permeability which is typical for dense thin graphene oxide films [26].

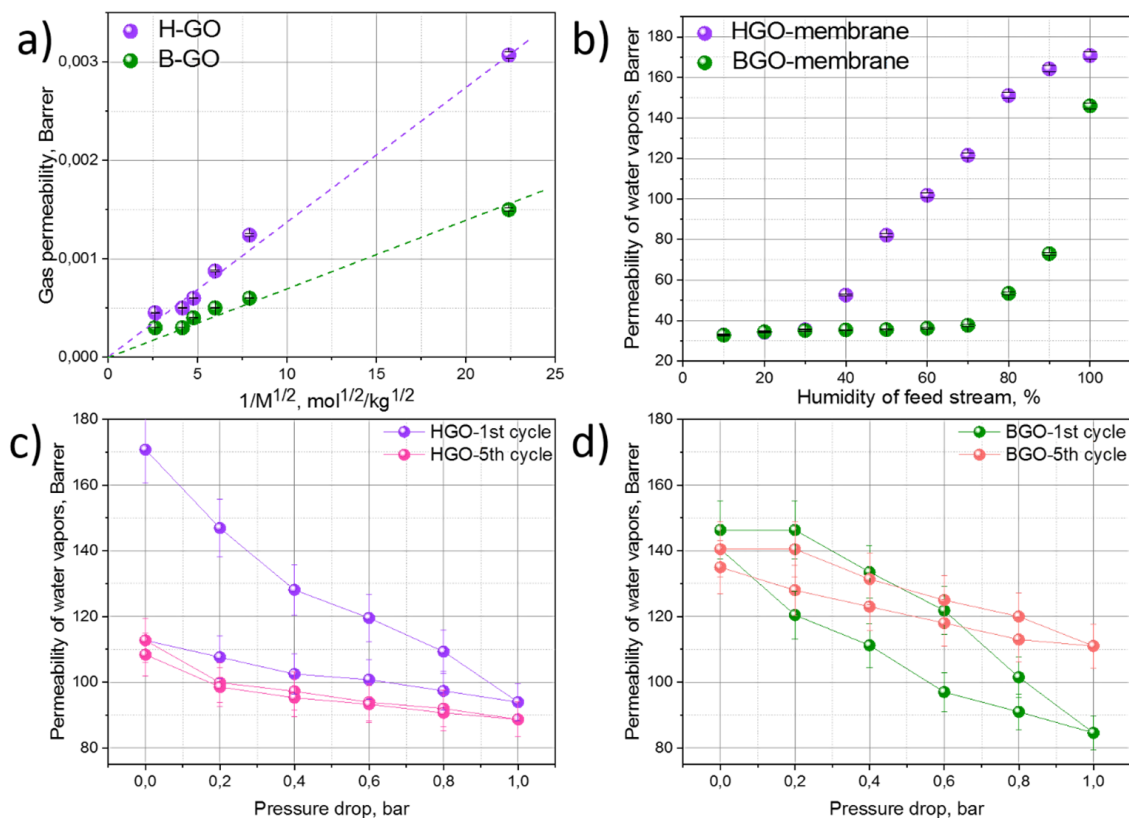


FIG. 3. Transport characteristics of composite membranes based on two types of graphene oxide: H-GO (Hummer' method) and B-GO (Brodie method): a) permeability of permanent gases: SF_6 , C_4H_{10} , CO_2 , N_2 , CH_4 , H_2 ; b) permeability of water vapors in the relative humidity range (RH) from 10 to 100 %; c), d) pressure stability of: c) H-GO and b) B-GO composite membranes in the range of pressure drop from 0 to 1 bar. The first and the fifth pressure cycle are shown

The H-GO and B-GO membranes exhibit relatively high water vapors permeability staying in the range of 30 – 170 Barrer depending on the humidity of the feed stream (Fig. 3(b)). It should be noted that in the low humidity range (up to 30 – 40 %), both H-GO and B-GO films have very close values of permeability, whereas, starting from humidity of 40 %, the permeability of H-GO begins to increase rapidly while the water vapor transport across B-GO remains small enough until the humidity of 80 % at which the B-GO permeability begins to increase sharply. The different shapes of water vapor permeability curves for H-GO and B-GO are evident and could arise from the difference in microstructure and chemical composition of the films. The high oxidation degree of H-GO and deep extent of oxidation (the high presence of C=O groups) favors the sorption and capillary condensation of water molecules in H-GO microstructure [22], thus, resulting in higher water vapor permeability in the humidity range of gas stream from 40 up to 100 %. In contrast, graphene oxide prepared by the Brodie method has greater C/O ratio with smaller amount of oxygen functional groups resulting in more rigid microstructure and lower water vapor permeability.

The prominent difference in the H-GO and B-GO membranes performance could be seen when the membranes are subjected to stepwise pressure cycling with pressure drops in the range from 0 to 1 bar (step of 0.2 bar) during water vapor permeability testing at 100 % humidity (Fig. 3(c,d)). During the first pressure cycle, the H-GO membrane loses up to 46 % of its original permeability, and, after pressure release, the membrane reveals an irreversible permeability decrease of ~30 %. The observed strong decrease in membrane permeability could be attributed to highly-oxidized and soft nature of nanoflakes in H-GO membrane which tend to compaction under pressure elevation resulting in shrinking the pathways

for water molecules transport. Nearly the same trend is observed for the B-GO membrane, however, it has higher stability: after the pressure release, the membrane restores its permeability with the irreversible loss of only $\sim 4\%$ revealing more rigid and stable microstructure of the B-GO compared to H-GO membrane. During further pressure cycling, the H-GO and B-GO membranes reveal stabilization of water vapor permeability. Under the 5-th pressure cycle, both H-GO and B-GO membranes exhibit the dynamical pressure decrease of $\sim 20\%$ with irreversible pressure loss of $\sim 4\%$ showing some kind of a limit in structural compaction of GO (Fig. 3(c,d)). The same trend for gradual compaction and stabilization of microstructure was shown for the permeation of H-GO membranes towards liquid water in nanofiltration experiments [27]. It could be assumed, that the observed difference in pressure stability in H-GO and B-GO is encoded in their synthesis method which pre-determines the extent of graphite oxidizing and the resulting defect content and rigidity of GO nanoflakes. To achieve enhanced pressure stability of graphene oxide, its microstructure should be close to that of B-GO membranes but with higher content of basal hydroxyl and epoxy groups to provide higher water vapor permeability. Thus, for the design of pressure-stable and highly-permeable membranes, the protocol of GO synthesis should be reconsidered carefully to avoid strong over-oxidation and defects formation in GO samples. The obtained results show that it could be possible to achieve pressure-stable GO using only microstructure-composition interplay as is shown for the B-GO membrane. This route could be considered as an alternative to modification of GO with various pressure-resistant agents such as, for instance, carbon nitride layers [6] or single-walled carbon nanotubes [7] to avoid complication of GO preparation for industry.

It should be noted that the performance of GO membranes under pressure requires further in-depth experimental studying including in-situ and operando X-ray diffraction analysis of d-spacing changing during pressure cycling which requires more sophisticated equipment. At present, most of the studies report the liquid (or vapor) water permeability under the average feed stream pressures in the range of 1 [28] to 6 bar [29] and even up to 50 bar [30], whereas the size of d-spacing for GO membranes is commonly measured and presented for the pressure of 1 bar. As a result, it is hard to correlate the membrane performance with dynamical pathways for water molecules transport in GO microstructure.

4. Conclusions

Gas and vapor transport characteristics as well as the resistance towards pressure drops is studied comparatively for membranes based on graphene oxide synthesized by Hummers' (H-GO) and Brodie's (B-GO) methods. It is revealed that B-GO membrane exhibits stronger resistance towards elevated pressure owing to higher uniformness of its microstructure provided by more rigid, less defective and lower oxidized planar nanoflakes. To enhance the pressure stability of graphene oxide, a careful control of synthesis conditions is required to provide the balance between GO oxidation degree and the rigidity of its nanoflakes. Thus, it is possible to control the pressure resistance of GO by adjusting its composition-microstructure interplay which could be considered as an alternative approach rather than introducing additional pressure-stabilizing agents.

References

- [1] Kim J.H. Grand Challenges in Membrane Applications—Gas and Vapor. *Frontiers in Membrane Science and Technology*, 2022, **1**.
- [2] Alen S.K., Nam S., Dastgheib S.A. Recent Advances in Graphene Oxide Membranes for Gas Separation Applications. *Int. J. of Molecular Sciences*, 2019, **20** (22), 5609.
- [3] Marcano D.C., Kosynkin D.V., Berlin J.M., Sinitskii A., Sun Z., Slesarev A., Alemany L.B., Lu W., Tour J.M. Improved Synthesis of Graphene Oxide. *ACS Nano*, 2010, **4** (8), P. 4806–4814.
- [4] Dreyer D.R., Park S., Bielawski C.W., Ruoff R.S. The chemistry of graphene oxide. *Chem. Soc. Rev.*, 2010, **39** (1), P. 228–240.
- [5] Wei N., Peng X., Xu Z. Understanding Water Permeation in Graphene Oxide Membranes. *ACS Applied Materials & Interfaces*, 2014, **6** (8), P. 5877–5883.
- [6] Liu L., Zhou Y., Xue J., Wang H. Enhanced antipressure ability through graphene oxide membrane by intercalating g-C₃N₄ nanosheets for water purification. *AIChE J.*, 2019, **65**, (10), e16699.
- [7] Han Y., Jiang Y., Gao C. High-Flux Graphene Oxide Nanofiltration Membrane Intercalated by Carbon Nanotubes. *ACS Applied Materials & Interfaces*, 2015, **7** (15), P. 8147–8155.
- [8] Tang X., Qu Y., Deng S.-L., Tan Y.-Z., Zhang Q., Liu Q. Fullerene-regulated graphene oxide nanosheet membranes with well-defined laminar nanochannels for precise molecule sieving. *J. Mater. Chem. A*, 2018, **6** (45), P. 22590–22598.
- [9] Li W., Zhang Y., Su P., Xu Z., Zhang G., Shen C., Meng Q. Metal-organic framework channelled graphene composite membranes for H₂/CO₂ separation. *J. Mater. Chem. A*, 2016, **4** (48), P. 18747–18752.
- [10] Huang H., Song Z., Wei N., Shi L., Mao Y., Ying Y., Sun L., Xu Z., Peng X. Ultrafast viscous water flow through nanostrand-channelled graphene oxide membranes. *Nature Communications*, 2013, **4**, 2979.
- [11] Yang R., Fan Y., Yu R., Dai F., Lan J., Wang Z., Chen J., Chen L. Robust reduced graphene oxide membranes with high water permeance enhanced by K⁺ modification. *J. of Membrane Science*, 2021, **635**, 119437.
- [12] Brodie B.C. XIII. On the atomic weight of graphite. *Philosophical Transactions of the Royal Society of London*, 1859, **149**, P. 249–259.
- [13] Staudenmaier L. Verfahren zur Darstellung der Graphitsäure. *Berichte der deutschen chemischen Gesellschaft*, 1898, **31** (2), P. 1481–1487.
- [14] Hofmann U., König E. Untersuchungen über Graphitoxyd. *Zeitschrift für anorganische und allgemeine Chemie*, 1937, **234** (4), P. 311–336.
- [15] Hummers W.S., Offeman R.E. Preparation of Graphitic Oxide. *J. of the American Chemical Society*, 1958, **80** (6), 1339.
- [16] Yoo M.J., Park H.B. Effect of hydrogen peroxide on properties of graphene oxide in Hummers method. *Carbon*, 2019, **141**, P. 515–522.
- [17] Talyzin A., Mercier G., Klechikov A., Hedenström M., Johnels D., Wei D., Cotton D., Opitz A., Moons E. Brodie vs Hummers graphite oxides for preparation of multi-layered materials. *Carbon*, 2017, **115**, P. 430–440.

- [18] Ibrahim A.F.M., Banihashemi F., Lin Y.S. Graphene oxide membranes with narrow inter-sheet galleries for enhanced hydrogen separation. *Chemical Communications*, 2019, **55** (21), P. 3077–3080.
- [19] Pedrosa M., Da Silva E.S., Pastrana-Martínez L.M., Drazic G., Falaras P., Faria J.L., Figueiredo J.L., Silva A.M.T. Hummers' and Brodie's graphene oxides as photocatalysts for phenol degradation. *J. of Colloid and Interface Science*, 2020, **567**, P. 243–255.
- [20] Eckmann A., Felten A., Mishchenko A., Britnell L., Krupke R., Novoselov K.S., Casiraghi C. Probing the Nature of Defects in Graphene by Raman Spectroscopy. *Nano Letters*, 2012, **12** (8), P. 3925–3930.
- [21] King A.A.K., Davies B.R., Noorbehesht N., Newman P., Church T.L., Harris A.T., Razal J.M., Minett A.I. A New Raman Metric for the Characterisation of Graphene oxide and its Derivatives. *Scientific Reports*, 2016, **6**, 19491.
- [22] Chernova E.A., Petukhov D.I., Chumakov A.P., Kirianova A.V., Sadilov I.S., Kapitanova O.O., Boytsova O.V., Valeev R.G., Roth S.V., Eliseev Ar., Eliseev An. The role of oxidation level in mass-transport properties and dehumidification performance of graphene oxide membranes. *Carbon*, 2021, **183**, P. 404–414.
- [23] Zhu Y., Murali S., Cai W., Li X., Suk J.W., Potts J.R., Ruoff R.S. Graphene and Graphene Oxide: Synthesis, Properties, and Applications. *Advanced Materials*, 2010, **22** (35), P. 3906–3924.
- [24] Reinecke S.A., Sleep B.E. Knudsen diffusion, gas permeability, and water content in an unconsolidated porous medium. *Water Resources Research*, 2002, **38** (12), P. 15–16.
- [25] Do D.D. Adsorption Analysis: Equilibria and Kinetics. In: *Series on Chemical Engineering*. Imperial College Press 1998, P. 892.
- [26] Nair R.R., Wu H.A., Jayaram P.N., Grigorieva I.V., Geim A.K. Unimpeded Permeation of Water Through Helium-Leak-Tight Graphene-Based Membranes. *Science*, 2012, **335** (6067), P. 442–444.
- [27] Chong J.Y., Wang B., Li K. Water transport through graphene oxide membranes: the roles of driving forces. *Chemical Communications*, 2018, **54** (20), P. 2554–2557.
- [28] Zhang Z., Xiao X., Zhou Y., Huang L., Wang Y., Rong Q., Han Z., Qu H., Zhu Z., Xu S., Tang J., Chen J. Bioinspired Graphene Oxide Membranes with pH-Responsive Nanochannels for High-Performance Nanofiltration. *ACS Nano*, 2021, **15** (8), P. 13178–13187.
- [29] Li Y., Zhao W., Weyland M., Yuan S., Xia Y., Liu H., Jian M., Yang J., Easton C.D., Selomulya C., Zhang X. Thermally Reduced Nanoporous Graphene Oxide Membrane for Desalination. *Environmental Science & Technology*, 2019, **53** (14), P. 8314–8323.
- [30] Wang Z., Ma C., Xu C., Sinquefeld S.A., Shofner M.L., Nair S. Graphene oxide nanofiltration membranes for desalination under realistic conditions. *Nature Sustainability*, 2021, **4** (5), P. 402–408.

Submitted 24 November 2022; revised 9 February 2023; accepted 1 April 2023

Information about the authors:

Ekaterina A. Chernova – Lomonosov Moscow State University, Faculty of Materials Science, 119991, Moscow, GSP-1, 1-73 Leninskiye Gory, Russia; Tula State University, 300012, Tula, Lenina avenue 92, Russia; ORCID 0000-0002-5812-9515; chernova.msu@gmail.com

Konstantin E. Gurianov – Lomonosov Moscow State University, Faculty of Materials Science, 119991, Moscow, GSP-1, 1-73 Leninskiye Gory, Russia; gurianovke@yandex.ru

Victor A. Brotsman – Lomonosov Moscow State University, Faculty of Chemistry, 119991, Moscow, GSP-1, 1-3 Leninskiye Gory, Russia; ORCID 0000-0002-8374-9265; brotsman.va@mail.ru

Rishat G. Valeev – Udmurt Federal Research Center of the Ural Branch of Russian Academy of Sciences (UdmFRC of UB RAS), Izhevsk, st. them. Tatiana Baramzina 34, 426067, Russia; ORCID 0000-0001-8981-8527; rishatvaleev@mail.ru

Olesya O. Kapitanova – Lomonosov Moscow State University, Faculty of Chemistry, 119991, Moscow, GSP-1, 1-3 Leninskiye Gory, Russia; ORCID 0000-0002-7384-3426; olesya.kapitanova@gmail.com

Mikhail V. Berekchiian – Lomonosov Moscow State University, Faculty of Materials Science, 119991, Moscow, GSP-1, 1-73 Leninskiye Gory, Russia; mikhail.berekchiyan@yandex.ru

Alexei V. Lukashin – Lomonosov Moscow State University, Faculty of Materials Science, 119991, Moscow, GSP-1, 1-73 Leninskiye Gory, Russia; alexey.lukashin@gmail.com

Conflict of interest: all authors declare that they have no potential conflict of interests.